

# Fabrication and characterization of chitosan/gelatin porous scaffolds with predefined internal microstructures

He Jiankang, Li Dichen\*, Liu Yaxiong, Yao Bo, Lu Bingheng, Lian Qin

State key lab for manufacturing systems engineering, Xi'an Jiaotong University, Xi'an 710049, China

Received 11 January 2007; received in revised form 10 May 2007; accepted 16 May 2007  
Available online 25 May 2007

## Abstract

The fabrication process for a novel three-dimensional (3D) chitosan/gelatin scaffold with predefined multilevel internal architectures and highly porous structures is presented combining solid freeform fabrication (SFF), microreplication and lyophilization techniques. The computer model of the scaffold is designed with biological data such as branching angle in liver vascular cast incorporated. Stereolithography (SL), known as a SFF technique, is utilized to build the resin mould, based on which poly-dimethylsilicone (PDMS) mould is produced by microreplication. The chitosan/gelatin hybrid solution is then cast onto the PDMS mould for pre-freeze and the monolayer porous structures with organized internal morphology are produced upon lyophilization. The 3D scaffold can be constructed via stacking these monolayer structures. The properties of porous structure, such as porosity, pore size and micromorphology as well as wall thickness, were investigated. Scanning electron microscopy (SEM) demonstrated that the scaffold possesses multilevel organized internal morphologies including vascular systems (portal vein, artery and hepatic vein) and parenchymal component (hepatocyte chamber). These organized structures enable orderly arrangement of hepatocyte and hepatic nonparenchymal cells and co-culture in the same 3D scaffold to guide liver regeneration in a controlled manner. Cell culture experiment *in vitro* showed that hepatocytes perform better in the well-defined chitosan/gelatin scaffold than in porous scaffold. This approach makes it flexible to investigate the relationship between internal scaffold microstructure and hepatocyte behavior *in vitro*. It also provides a new way to fabricate complex 3D scaffold using various natural biomaterials for vital organ engineering.

© 2007 Elsevier Ltd. All rights reserved.

**Keywords:** Predefined channels; Porous; Chitosan/gelatin

## 1. Introduction

The severe donor shortage of orthotopic allogeneic livers and the extremely high transplantation cost have stimulated continuing efforts to develop a tissue-engineered liver by growing hepatic cells [1]. In this way, three-dimensional (3D) scaffold is commonly necessary to provide the initial extracellular matrix (ECM) to support the cells and may also determine hepatic cell morphology and function as well as the micro- or macro-structure of the tissue-engineered liver [2,3]. As a rich vascularized organ, liver tissue-engineered scaffold should be endowed with some specific characteristics:

(1) surface chemistry to favor cellular attachment, differentiation and proliferation; (2) biodegradability to match new tissue regeneration ratio; (3) interconnected porous structures so as to facilitate nutrient and oxygen delivery and waste removal; (4) predefined internal vascular channels to support thick liver tissue regeneration and vascularization and (5) nontoxicity for the scaffold materials and their by-products.

To engineer porous scaffolds, several processing techniques have been developed such as freeze drying [4–8] and salt leaching [9]. These techniques enable to create highly porous structures with porosity 90% ~ 95%. However, they are dependent on a randomly distributed pore generation mechanism, which cannot precisely control the pore size and distribution, ensure reliable interconnection [10] and produce a predefined internal architecture within to favor angiogenesis. In addition, these foam structures could only result in the growth of thin

\* Corresponding author. Tel.: +86 029 82665575; fax: +86 029 82660114.  
E-mail address: [dcli@mail.xjtu.edu.cn](mailto:dcli@mail.xjtu.edu.cn) (L. Dichen).

cross-sections of tissue limited by the mass transfer properties of the scaffold material [11,12]. Even if the porosity is fully interconnected, cells cannot migrate deep into the scaffold because of the lack of nutrients and oxygen along with insufficient removal of waste products [13]. Some researches show that, without an intrinsic capillary network, the maximal thickness of engineered tissue is approximately 150–200  $\mu\text{m}$  [14,15]. Thus, creating predefined internal vascular channels is crucial to the growth of thick cross-sections of liver tissue.

Solid freeform fabrication (SFF) techniques, via layer-by-layer process, make it possible to produce liver tissue-engineered scaffolds with predefined and reproducible internal microstructures, which could serve as an artificial vascular system. In particular, 3D printing (3DP) has been used to create porous synthetic polymer scaffolds [16]. Chloroform as the binder was ejected onto polylactic acid (PLA) or polylactico-glycolic acid (PLGA) powders containing salt particles (45–150  $\mu\text{m}$  in diameter) to create liver tissue-engineered scaffolds. The fabricated interconnected channels have an approximate diameter of 800  $\mu\text{m}$  and the minimum wall thickness between random micropores is claimed to be 200  $\mu\text{m}$ , which was intended to facilitate oxygen and nutrients delivery along with waste removal [17,18]. However, any residual chloroform in the scaffold would be toxic to the cells. Furthermore, the surface chemistry of these synthetic polymers does not promote cell adhesion and the acidic environment resulting from their degradation by-products may induce an adverse inflammatory response [19,20].

Microfabrication technique, known as microelectromechanical systems (MEMS), has also been utilized to construct liver tissue-engineered scaffolds. This approach could create almost all the physiological length scales from capillaries to large vessels. Some researchers [21] etched branching vascular and capillary network on silicon and Pyrex wafers, on which hepatocytes and endothelial cells were cultured, respectively. Hepatocyte sheets were lifted off, folded into compact 3D configurations and implanted into rat omenta, resulting in the formation of vascularized hepatic tissue. Poly-dimethylsilicone (PDMS) templates by replica-moulding from micromachined silicon wafers with vascular networks were used to culture endothelial cells *in vitro* and the result showed that the endothelial cells could grow to near confluence in the confined microchannels [22]. However, to realize *in vitro* artificial liver tissue for implantation applications [23,24], these devices are not suitable because they are not biodegradable. Although microfabricated biodegradable polymer scaffolds have been used for hepatocytes or endothelial cells culture [25,26], these approaches involve either expensive MEMS equipments or special photosensitive biodegradable polymers.

Chitosan and gelatin are interesting biomaterial candidates due to their good biocompatibility, biodegradability, low toxicity and low cost, and their composite has a wide spectrum of tissue engineering applications, such as drug carriers, bone, nerve repair and hepatocytes culture [27–32]. Studies show that hepatocytes could attach and proliferate on the porous chitosan scaffold [33,34]. However, to date, chitosan/gelatin scaffolds have been fabricated into foam structures mostly via freeze drying

technique. Therefore, the limitation on mass transfer in these porous structures still exists.

In the present study, we sought to develop a novel fabrication process for chitosan/gelatin composed liver tissue-engineered scaffolds with well-defined internal morphology by combining SFF, microreplication and freeze drying techniques. Stereolithography (SL) system was employed to fabricate the resin moulds, based on which the PDMS templates were microreplicated. The chitosan/gelatin solution was then cast into the PDMS templates and the porous scaffold with predefined channels was produced using freeze drying technique. Hepatocyte performance on the resultant scaffold was investigated *in vitro*. These monolayer scaffolds could be further stacked together using original chitosan/gelatin solution and potentially be applied to microfabricate implantable 3D scaffolds of specified architecture. Through this strategy, it is easy to investigate the effect of different internal microstructures in 3D scaffold on hepatocyte behavior *in vitro* and *in vivo*.

## 2. Materials and methods

### 2.1. Materials

Chitosan was purchased from Sanland Chemicals Co. (USA). The degree of deacetylation was 92%. Gelatin was obtained from Sino-American Biotechnology Co. (Luoyang, China). The liver vascular cast was generously provided by the Institute of General Surgery, General Hospital of PLA in China. All other reagents were local products of analytical grade.

### 2.2. Chitosan/gelatin solution formulation

Chitosan and gelatin solutions with various concentrations were prepared by dissolution in 1 wt% acetic acid. The two solutions were mixed at 1:1 ratio (v/v) under agitation for 12 h at 37 °C, then degassed in vacuum for 2 h to form uniform solution (Table 1). Glutaraldehyde solution of 0.5 ml and 0.25 wt% was incorporated into 16 ml mixture to crosslink chitosan/gelatin solution.

### 2.3. Fabrication process

Fig. 1 summaries the fabrication process of liver tissue-engineered scaffold. The computer mould was designed using commercial CAD software (Pro/Engineer wildfire, PTC). In order to incorporate biological data into the mould design, we obtained the vascular cast of a liver tissue (rat). The method could be reviewed as follows [35]: a liquid plastic was injected into the blood vessels of the liver. Once the plastic had solidified, liver tissue was dissolved, leaving a solid

Table 1  
Formulation of chitosan and gelatin mixture solution

Chitosan solution (wt%)	0.5%	1.0%	1.5%	2.0%	2.5%	3.0%
Gelatin solution (wt%)	1.7%	3.3%	5.0%	6.7%	8.3%	10%
Chitosan/gelatin solution (v/v)	C/G1	C/G2	C/G3	C/G4	C/G5	C/G6

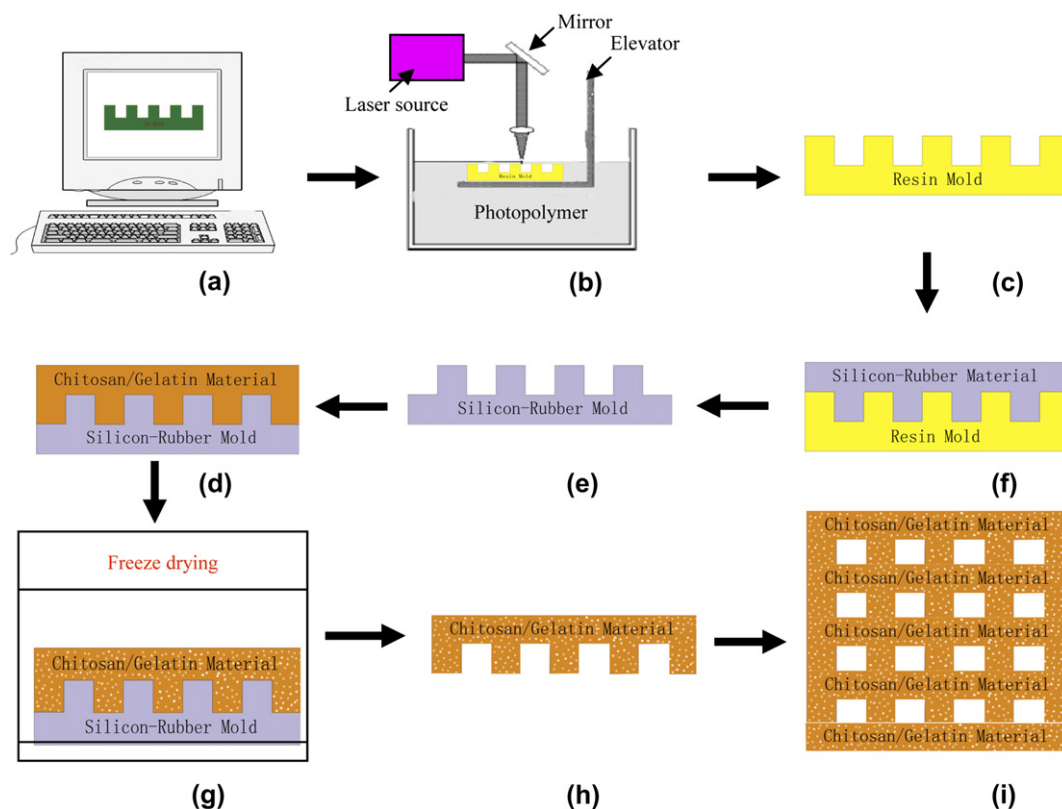


Fig. 1. Schematic of fabrication process. (a) 3D computer mould, (b) resin scaffold prototype made by SL apparatus, (c) finished resin mould with predefined internal structure, (d) PDMS mould produced by microreplication technique, (e) completed PDMS negative mould, (f) chitosan/gelatin mixture solution cast onto the PDMS mould, (g) the chitosan/gelatin mixture pre-frozen at  $-60^{\circ}\text{C}$  and lyophilized, (h) a dry chitosan/gelatin scaffold and (i) single-layer scaffold.

cast of the organ's blood vessels. The branching angles of these vessels were measured microscopically and analyzed statistically. The optimum branching angle was selected and incorporated into the mould design.

The computer mould was fabricated with a commercial SL apparatus, SPS 600 (Institute of Advanced Manufacturing Technology in Xi'an Jiaotong University, China). Fabricating each layer consists of a filling process and a cross-section fabrication process. The filling process is to form a new liquid layer of photopolymer on the solidified surface. For the fabrication of a cross-section, a laser beam, focused into a spot with approximately  $100\ \mu\text{m}$  in diameter, is irradiated on the open surface of liquid photopolymer. Polymerization is initiated by the photons and then the irradiated photopolymer becomes solidified. After one layer is finished, the elevator goes down and a new liquid photopolymer layer is formed. By repeating the above process, a complex 3D structure can be obtained.

PDMS mould was prepared by mixing the commercially available polymer and catalyzer in a 100:2 ratio by weight. The mixture was degassed under vacuum to eliminate bubbles. Then the mixture was cast on the resin mould and placed under vacuum to remove bubbles once again. PDMS was placed statically at room temperature for 4 h and then peeled from the resin mould. The PDMS mould was then washed with 90% ethanol and sonicated for 5 min prior to use.

The chitosan/gelatin mixture solution is then cast into the PDMS mould. Due to the hydrophobic property of PDMS

material, it is difficult for the solution to fill the small chambers between predefined internal channels and repeated vacuum is needed. The PDMS mould is then placed in a refrigerator or liquid nitrogen with the pre-frozen temperatures at  $-20^{\circ}\text{C}$ ,  $-60^{\circ}\text{C}$ ,  $-90^{\circ}\text{C}$ ,  $-180^{\circ}\text{C}$  for 4 h. The frozen mixtures were lyophilized within a freeze-dryer (DTY-1SL, China) for 36 h. The porous scaffolds were washed with distilled water and then treated using previously described method [30].

To create 3D scaffolds, these single-layer structures should be stacked together. As far as the interface between scaffolds with the host tissue or bioreactor was concerned, special interface scaffold should be custom designed and fabricated to provide uniform inlet and outlet channels. For stacking, single-layer structures are manipulated with tweezers and a thin layer of water mist was spurted onto the surface of the first structure. The lyophilized chitosan/gelatin material was enabled to be slightly dissolved locally and the next layer was stacked onto the top of the first structure by manual positioning. After the whole assembly was completed by repeating the abovementioned procedure, it was frozen and lyophilized to make a permanently glued 3D scaffold.

#### 2.4. Precision of fabrication process

The precision of the fabrication process was evaluated by measuring the different length scales of resin mould, PDMS mould and the final chitosan/gelatin scaffold using optical

microscopy (KEYENCE VH-Z450, Japan) in comparison with the designed dimension accordingly. The dimension values range from 200  $\mu\text{m}$  to 500  $\mu\text{m}$ . Not less than ten measured values were obtained for each dimension of the three kinds of sample. The branching angle incorporating into the scaffold was also measured.

### 2.5. Microstructural characterization

The scaffolds with predefined internal microstructures were characterized by scanning electron microscopy (SEM, HITACHI S-3000N). The micropores were revealed by immersing the scaffold into liquid nitrogen for several seconds and sectioning with a razor blade. The surface with predefined internal microstructures and the cross-sections were coated with Au prior to SEM observation (JEOL, JEE-420). The size of micropores prepared under different pre-frozen temperatures as well as the wall thickness at the magnification of  $\times 800$  were measured. At least ten pores were assessed from three different areas of the same sample.

### 2.6. Porosity

The porosity of the porous chitosan/gelatin scaffolds with different concentrations was measured by liquid displacement [9,36,37]. Ethanol was selected as the displacement liquid as it permeates through the scaffolds without swelling or shrinking the matrix. The scaffolds (dry weight,  $W_d$ ) were immersed in the ethanol under vacuum for 5 min and the weights of scaffolds in ethanol were recorded as  $W_1$ . The scaffolds were taken out and the liquid on the surface was removed by filter paper. The weight of the wet scaffold was recorded as  $W_w$ . The porosity of the chitosan/gelatin scaffold could be obtained by:

$$\varepsilon(\%) = \frac{(W_w - W_d)}{(W_w - W_1)} \times 100\%$$

### 2.7. Scaffold postprocessing

If newly lyophilized chitosan/gelatin scaffolds were rehydrated in a neutral aqueous medium, they exhibited rapid swelling and ultimately dissolved, which results from the residual acetic acid. This indicated that before application in tissue engineering, the lyophilized structures should be postprocessed including neutralizing and crosslinking. In the current study, the scaffolds ( $W_{\text{orig}}$ ) were neutralized by rehydrating in either dilute NaOH (0.1 M), or in an ethanol series such as 100%, 70%, and 50%, and then washed with distilled water. The neutralized samples were lyophilized and then weighed as  $W_{\text{neut}}$ . The dimension change and the weight loss ratio were investigated. The weight loss ratio could be calculated as follows:

$$\text{Weight loss ratio} = \frac{(W_{\text{orig}} - W_{\text{neut}})}{W_{\text{orig}}} \times 100\%$$

To improve the mechanical strength, crosslinking was conducted on the neutralized scaffolds. As far as the predefined

internal architectures were concerned, it is important to maintain the original morphology during crosslinking process. Therefore, two kinds of solvents, distilled water and absolute ethanol, were used to dilute glutaraldehyde into 0.25% solutions. Their effect on the morphology of the crosslinked chitosan/gelatin scaffolds was investigated, especially in terms of dimensional change. The scaffolds should be further treated with 5% sodium borohydride aqueous to block residual aldehyde groups. The swelling ratio of the scaffolds before and after crosslinking was calculated as:

$$\text{Swelling ratio} = \frac{(W_w - W_d)}{W_d} \times 100\%,$$

where  $W_d$  represents the weight of dry scaffold and  $W_w$  is the weight of wet scaffold.

### 2.8. Hepatocyte isolation and culture

Hepatocytes were isolated from male Sprague–Dawley rats, weighing 200–250 g by perfusion the liver with 0.05% collagenase according to the method of Puviani [38]. The isolated hepatocytes were washed twice with basal Williams' E medium and further purified by two centrifugations at 500 rpm for 3 min. The hepatocyte viability was above 90% assessed by Trypan blue exclusion.

The isolated hepatocytes were seeded at a density of  $1.0 \times 10^6$  cells/ml within the pre-organized porous scaffolds placed in the well of a 24-well tissue culture plate. After 1 ml culture medium was added, the cell-seeded scaffold were cultured in a humidified incubator at 37 °C in 5% CO<sub>2</sub> atmosphere, with daily medium changes. Hepatocyte morphology and proliferation behavior were investigated using SEM.

## 3. Results

### 3.1. Branching angle in liver vascular cast

The branching angles in the natural liver vascular cast were measured statistically using optical microscopy as shown in Fig. 2(a). It is assumed that the natural vascular branching angle can facilitate blood flow. Through statistical analysis ( $N = 133$ ), it is found that the branching angle distribution conforms approximately to the normal distribution (Fig. 2(b)). Most vascular branching angles range from 60° to 90° and the mean value is about 78°.

### 3.2. Fabrication precision

As shown in Fig. 3(a), the smallest feature produced by the novel fabrication process is  $187.7 \pm 16.5 \mu\text{m}$ , which was designed to have a dimension of 200  $\mu\text{m}$ . The dimensions of the predefined channels in the final porous scaffold are insignificant at the  $p < 0.01$  level compared to that in the resin mould, which are at the  $0.03 < p < 0.08$  level in comparison to the designed dimensions (200  $\mu\text{m}$ , 300  $\mu\text{m}$  and 480  $\mu\text{m}$ ). This indicates that the fabrication precision is mainly dependent on



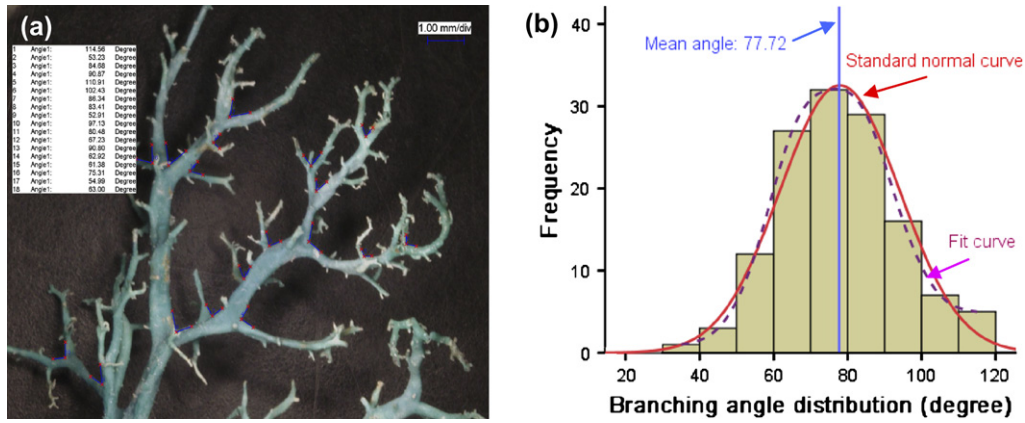


Fig. 2. Statistical analysis on the branching angle in liver vascular cast. (a) Vascular cast of rat's liver, (b) branching angle distribution with the mean angle about 78°.

precision of the resin mould, which is accordingly determined by the resolution of the SL apparatus.

In Fig. 3(b), the mean branching angle in the porous scaffold is about 79°, which was designed at 78° in the computer model. The value discrepancy was also mainly caused by the fabrication of resin mould. Fig. 3(c) and (d) is the SEM images of pre-fabricated channels. The arrows represent the flow directions in the scaffold and the branching angle was relatively accurately created.

### 3.3. Macro- or micromorphology

Fig. 4 shows the CAD model, resin mould and the chitosan/gelatin scaffold with specific macroscopic shape and predefined internal microarchitectures. It is designed for liver tissue-

engineered scaffold and the predefined features include portal vein, artery, hepatocyte chambers as well as hepatic vein (Fig. 4(a)). The blood could flow in via the six portal veins and arteries, mixed at the interconnected channels (simulating capillary network), and then flow out from the hepatic vein. The hepatocyte should be seeded into the hepatocyte chambers.

As shown in Fig. 4(d), the predefined features were accurately patterned. The smallest channels are approximately 150 μm in width and the smallest distance between channels and chambers is about 170 μm. The scales for the hepatocyte chambers are 200 μm in width and 580 μm in length. The volume between the blood vessels and the hepatic chambers is a fully interconnected porous structure as shown in Fig. 4(e) and (f), which were segmented longitudinally and transversely.

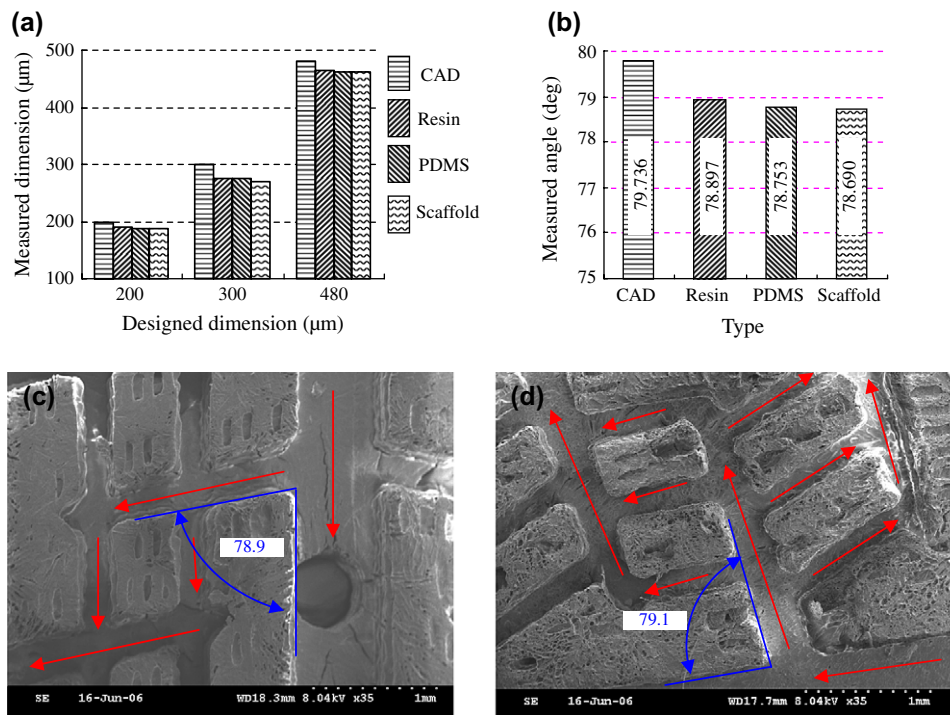


Fig. 3. The resolution of the novel presented fabrication process. (a) The measured dimension of resin mould, PDMS mould and final scaffold versus the designed dimension of CAD model, (b) the branching angles for CAD model, resin mould, PDMS mould and porous scaffold, (c) branching angle incorporated into the sample scaffold fabrication and (d) branching angle incorporated into the complex scaffold fabrication.

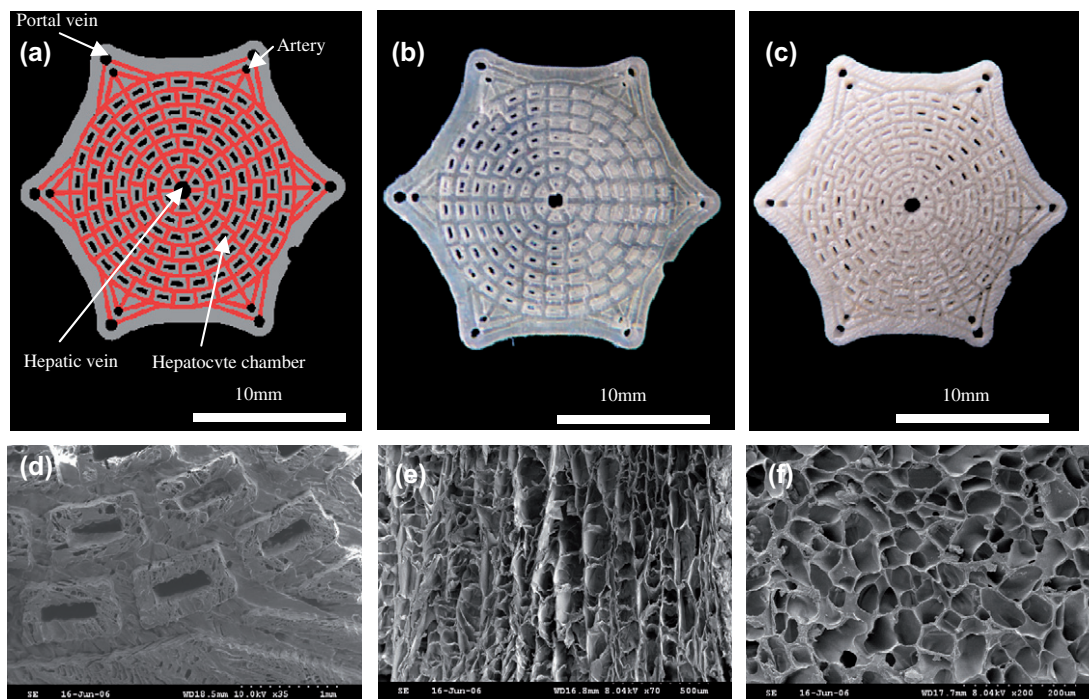


Fig. 4. Porous chitosan/gelatin scaffold with specific external shape and predefined internal morphology. (a) CAD model, (b) resin mould fabricated using SL technique, (c) porous chitosan/gelatin scaffold, (d) SEM of the predefined internal morphology, (e) microstructures when segmented longitudinally and (f) microstructures when segmented transversely.

### 3.4. The effect of concentration on porosity

The porosity of lyophilized scaffold produced from different concentrations of chitosan/gelatin solution is illustrated in Fig. 5. With the decrease in concentration, the porosity could increase from 90.62% to 98.13%. These highly porous structures could not only improve mass transfer rate of oxygen and nutrients into the inner pores, but also efficiently remove metabolic products [34].

However, when the solution was blended with 4% chitosan and 15% gelatin, it was too viscous to fill the small

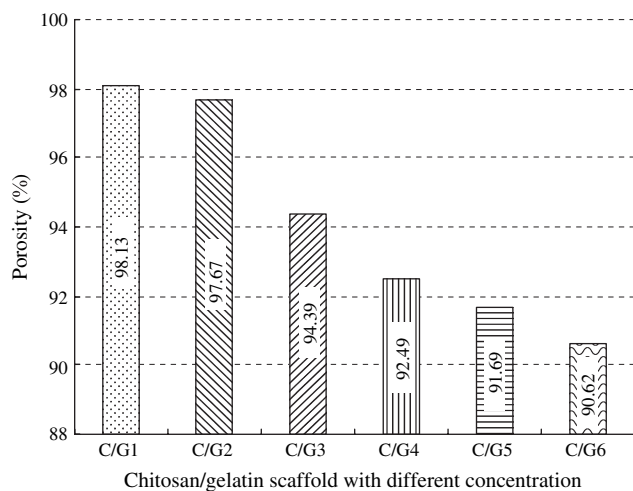


Fig. 5. The effect of concentration of chitosan/gelatin solution on the porosity of lyophilized scaffold (pre-freezing temperature: 60 °C).

trenches between the predefined channels on the PDMS mould, which would influence replication resolution significantly. On the other hand, when the solution was blended with 0.5% chitosan and 1.7% gelatin, the resultant scaffold was weak and deformable, which leads to the demolding process difficultly. Therefore, the optimal concentration of chitosan/gelatin solution should be controlled between C/G1 and C/G6 to produce a lyophilized scaffold with fine predefined morphology.

### 3.5. The effect of pre-freezing temperature on pore size and wall thickness

For porous scaffolds prepared by freeze drying method, pre-freezing temperature is an important factor to affect the mean pore size and wall thickness. As shown in Fig. 6(a), the mean pore size could be modulated from 17  $\mu\text{m}$  to 115  $\mu\text{m}$  by changing the pre-freezing temperature. The mean pore size becomes smaller along with lower pre-freezing temperature. The mean wall thickness of the porous scaffolds pre-frozen at  $-20$  °C,  $-60$  °C,  $-90$  °C and  $-180$  °C is illustrated in Fig. 6(b). It is clear that the pre-freezing temperature has little effect on the wall thickness ranging from 3.3  $\mu\text{m}$  to 5.2  $\mu\text{m}$  with the thinnest wall at  $-90$  °C.

The same conclusion could be drawn from the SEM pictures shown in Fig. 7. Each picture has the same size and magnification ( $\times 800$ ), but the number of pores increases from  $-20$  °C to  $-180$  °C, which indicates that at a lower temperature, the number of crystal nuclei initially formed is larger than that at a higher pre-freezing temperature.

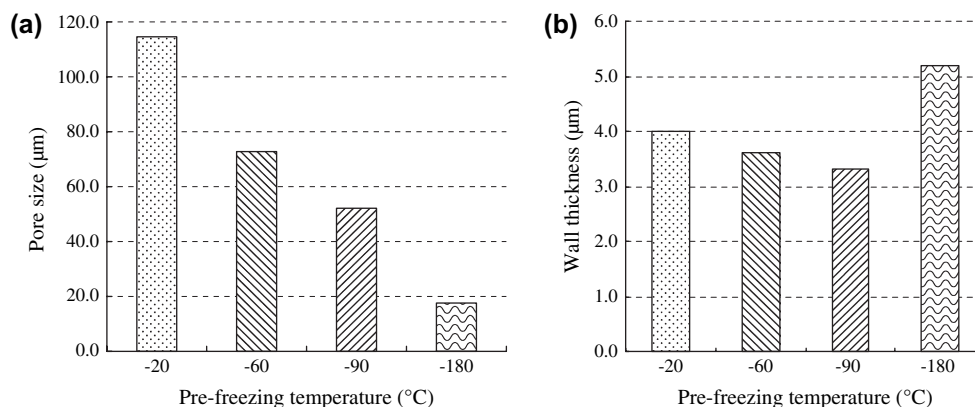


Fig. 6. The effect of pre-freezing temperature on pore size (a) and wall thickness (b).

### 3.6. Postprocessing

In Fig. 8(a), the overall dimension of the scaffolds was influenced by the neutralization solution. The scaffolds hydrated in NaOH exhibited some swelling (overall dimension from 1.83 cm to 2.12 cm), probably caused by base-induced changes in crystallinity and associated structural stress [39]. These changes were only partially reversed upon lyophilization. In comparison, the scaffolds hydrated through an ethanol series exhibited slight shape changes (overall dimension from 1.85 cm to 1.91 cm), which could be almost completely reversed after lyophilization. Fig. 8(b) shows that the weight loss of scaffold during neutralization process in ethanol series (10.13%) is smaller than that in NaOH (18.37%). Therefore,

the neutralized solution was selected as ethanol series unless otherwise mentioned.

After neutralization, the scaffolds were crosslinked in 0.25% glutaraldehyde solution and began to shrink as shown in Fig. 8(c). The scaffolds crosslinked in glutaraldehyde aqueous solution exhibit small shrinkage in overall dimension and these changes could reverse approximately to the original dimension of the scaffolds upon lyophilization. On the other hand, the scaffolds crosslinked in glutaraldehyde ethanol solution shrink severely and these changes are irreversible. The swelling ratio of the crosslinked scaffolds decrease largely in comparison with that of non-crosslinked scaffolds and the concentration of chitosan/gelatin also has a direct effect on the swelling ratio of the scaffold (Fig. 8(d)).

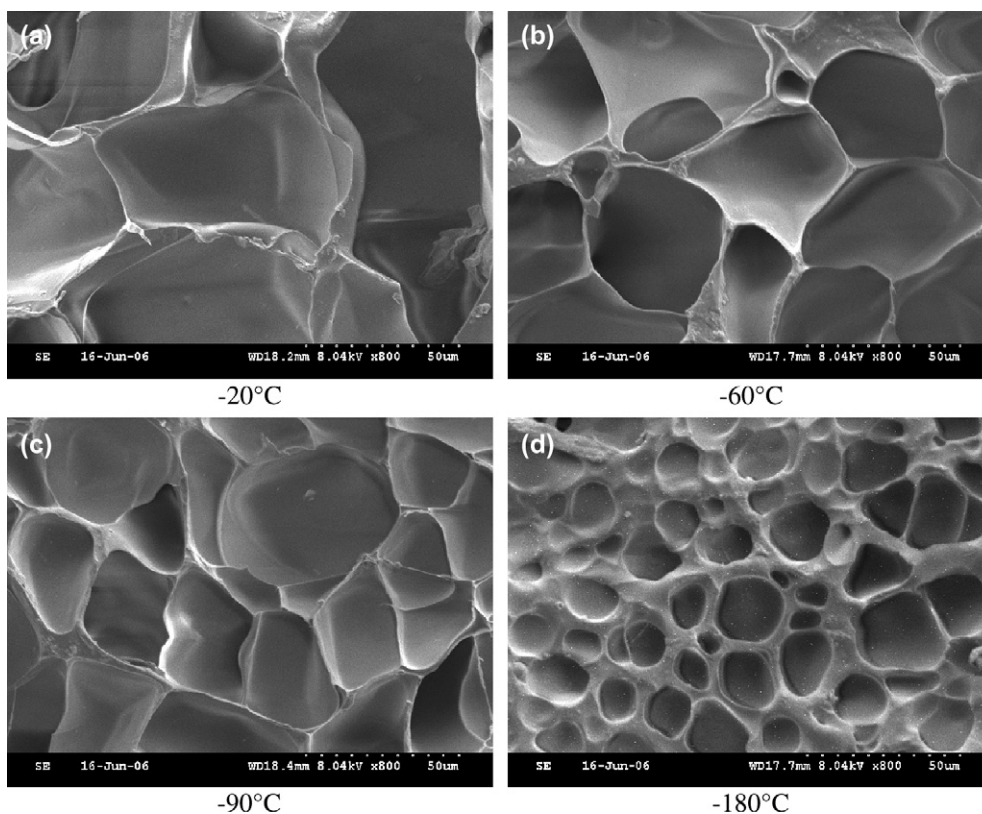


Fig. 7. SEM of the structure of chitosan/gelatin scaffold affected by pre-freezing temperature.



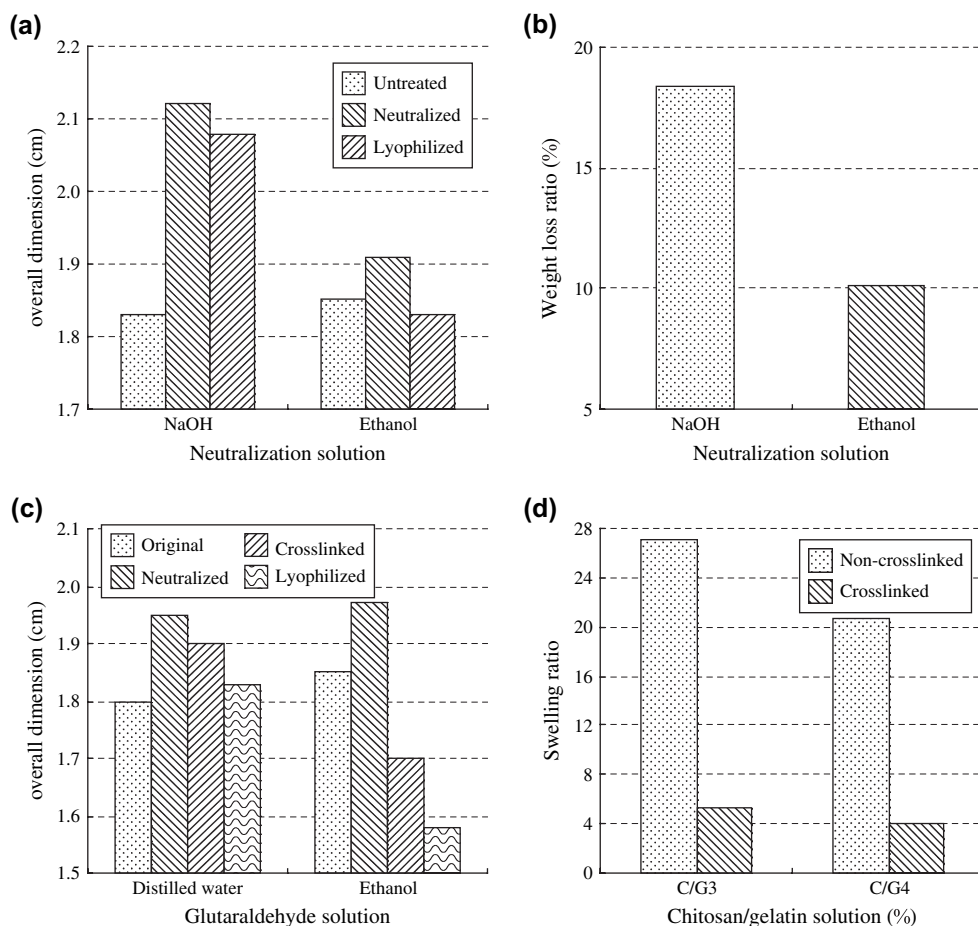


Fig. 8. The effect of postprocessing on the scaffold's properties. (a) The overall dimension influenced by different neutralized solution, (b) the weight loss ratio influenced by different neutralized solution, (c) the overall dimension influenced by different glutaraldehyde solution and (d) the swelling ratio for non- and cross-linked scaffolds produced from different concentrations.

### 3.7. Hepatocyte culture

The behavior of hepatocyte in porous chitosan/gelatin scaffold and well-defined chitosan/gelatin scaffold cultured for 1 day and 3 days was compared by SEM. When cultured for 1 day, the number of hepatocytes attached on the surface of porous scaffold (Fig. 9(a)) is relatively less than that of well-defined scaffold (Fig. 9(c)), and the secreta secreted by hepatocytes on the well-defined scaffold could be clearly distinguished from SEM picture. After 3 days, the hepatocytes proliferated better in well-defined scaffold than in porous scaffold, and the secreta have covered the total surface of the predefined channels. Although re-established hepatocytes cell–cell contacts can be seen in the porous scaffold (Fig. 9(b)), fewer cell aggregates were observed to form multicellular spheroids as seen in the well-defined scaffold (Fig. 9(d)). This result proved that high cell viability of hepatocytes could be obtained in the well-defined porous chitosan/gelatin scaffold when cultured *in vitro*.

### 3.8. Stacking of monolayer structures

To create the 3D porous scaffold, the monolayer structures and the special interface structures were stacked together. As

shown in Fig. 10(a) and (b), the monolayer structures could possess different predefined internal morphologies with the same macroscopic shape. The thickness of each single-layer structure is about 2 mm, but that of the 3D scaffold with seven layers is about 12.78 mm. The thickness of dissolved material between two layers is about 200  $\mu\text{m}$  in the stacking process. Fig. 10(c) reveals that the resultant 3D chitosan/gelatin scaffold and the internal microstructures are maintained pretty well as shown in Fig. 10(d). It is worthwhile to point out that, under perfusion condition, the culture media should afflux from the round channels in trench 1, collected into the trench 2 via the mid interconnected vessels and then flow out from the round channels in trench 2. Through this strategy, the culture media could flow uniformly throughout the 3D porous scaffold.

## 4. Discussion

To date, the most successful tissue engineering applications are skin and bladders, which have comparatively low requirements for nutrients and oxygen and can be supplied by the host vasculature [40–42]. But for the regeneration of liver, relying on host vascularization alone is not sufficient and pre-established vasculature is critical to enhance angiogenesis



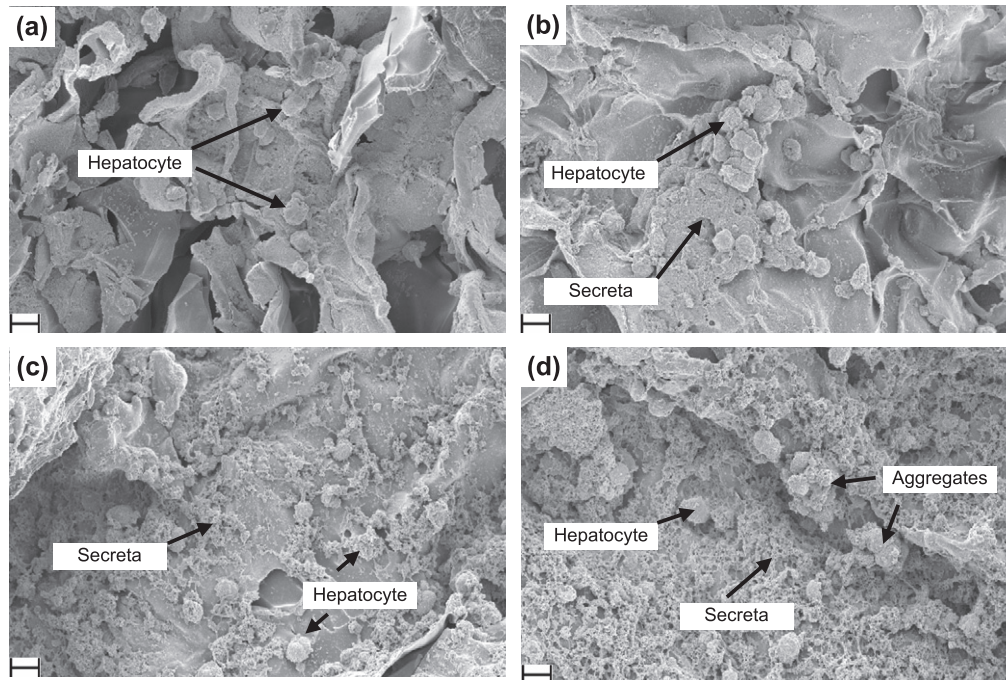


Fig. 9. SEM images of hepatocyte cultured within porous chitosan/gelatin scaffold: (a) 1 day; (b) 3 days and well-defined chitosan/gelatin scaffold: (c) 1 day; (d) 3 days. The scale bar indicates 10  $\mu\text{m}$ .

for hepatocytes long-term survival and proliferation. The improved performance of hepatocytes is mainly dependent on several factors: (1) stable 3D spatial microenvironment mimicking the natural liver [43], (2) pre-established vasculature bed for sufficient nutrients and oxygen delivery as well as timely waste removal, (3) cell–cell communication and biochemical cross-talk for the maintenance of differentiated cell functions [44], (4) integration of multiple cell types.

It has been evident that several liver-specific functions, such as albumin secretion and urea synthesis, could be maintained when hepatocytes are cultured on the 3D porous scaffold *in vitro* [45–49]. Improved performance of hepatocytes could also be obtained in the microfabricated patterns or chambers [50,51]. In addition, the need for angiogenesis or an established vasculature bed is evident by the success of the endothelial cells in the structures close to the culture medium. Our approach is to combine SFF, microreplication and freeze drying techniques to fabricate highly porous 3D chitosan/gelatin scaffolds (90–98%) with predefined internal channels. These

pre-fabricated internal channels in the 3D scaffold may be the key to successfully grow thick cross-sections of tissue because immediate oxygen and nutrients supply could be fulfilled before angiogenesis occurs [52,53]. The interconnected porous structure between these predefined channels could further enhance the mass transfer capacity deep into the scaffold. Furthermore, the pre-fabricated hepatic chambers are expected to provide the space for hepatocytes proliferation and aggregation.

Co-culture of hepatocytes with other kinds of cells could improve hepatocyte performance. Harada *et al.* [54] found that rat small hepatocytes could proliferate and rapidly form a hepatic organoid when co-cultured with hepatic nonparenchymal cells in collagen sponge. The albumin secretion of hepatocytes increased with time when co-cultured with fibroblasts on the patterned polyelectrolyte multilayer templates [55]. Enhanced liver functions of hepatocytes could be obtained when co-cultured with NIH 3T3 in the alginate/galactosylated chitosan scaffold [56]. Hepatocyte could maintain long-term survival

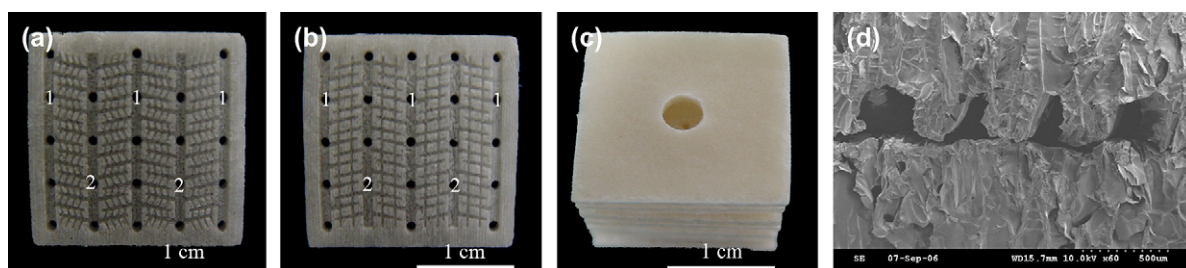


Fig. 10. 3D chitosan/gelatin scaffold stacked from single-layer structures. (a) Complex internal structures, (b) simple internal architectures, (c) macroscopic shape of 3D porous scaffold and (d) internal microstructures (50).

when co-cultured with endothelial cells in the 3D microfluidic scaffolds [57]. Our 3D scaffold could possess multilevel organized internal morphologies including vascular systems (portal vein, artery and hepatic vein) and parenchymal component (hepatic chamber). These organized architectures have the potential to enable various liver cells such as hepatocyte and endothelial cells orderly arrangement and co-culture in the same 3D scaffold and guide organ regeneration in a controlled manner. Thus, multiple-type liver cells co-culture that include appreciate heterotypic cell interactions in mimicking liver microarchitecture may ultimately be required to obtain the full spectrum of liver functions *in vitro*.

Although the cell culture experiment has shown that the hepatocytes express better performance in well-defined scaffold than in porous scaffold, the hepatocyte behavior within 3D stacked scaffold should be further investigated under perfusion condition and the co-culture experiment of hepatocyte with endothelial cells as well as other hepatic nonparenchymal cells is also needed to engineer a functional liver organoid. Furthermore, the assembly process for monolayer scaffolds should be further optimized, and the internal channel microarchitectures should be biomimetically reconstructed based on the microCT images of liver vascular cast.

## 5. Conclusion

The obtained chitosan/gelatin scaffold includes predefined multilevel internal architectures (vasculature bed and hepatocyte chamber) and highly porous structures (porosity above 90%). The pre-fabricated vascular system can supply immediate nutrients and oxygen and the porous structures can enhance the capacity of mass transfer. The porosity, pore size and morphology can be easily controlled and the optimal post-processing method was obtained to improve the wet performance of the scaffold. Cell culture *in vitro* showed that hepatocytes perform better in the well-defined scaffold than in porous scaffold. The fabrication method by stacking monolayer structures into 3D scaffold makes it possible to construct complex liver tissue engineering scaffold, even with biomimetic vascular system and anatomical external geometry. However, the stacking process needs to be optimized and further cell culture or co-culture experiment is required to verify the efficiency of using the 3D scaffolds to promote liver regeneration.

## Acknowledgements

The authors express their deepest gratitude to the Natural Science Foundation of China (50575170) the Research Fund for the Doctoral Program of Higher Education of China (No. 20050698002) and Shaanxi province scientific research key project (no.2006K06-G17). We would also like to acknowledge Professor Xu Yingxin from the Institute of General Surgery, General Hospital of PLA in China for supplying the liver vascular cast.

## References

- [1] Wang XH, Li DP, Wang WJ, Feng QL, Cui FZ, XU YX, et al. Cross-linked collagen/chitosan matrix for artificial livers. *Biomaterials* 2004; 24:3213–20.
- [2] Allen JW, Hassanein T, Bhatia SN. Advances in bioartificial liver devices. *Hepatology* 2001;34(3):447–55.
- [3] Langer R, Vacanti JP. Tissue engineering. *Science* 1993;260:920–6.
- [4] Mooney DJ, Karfmann PM, Sano K, Mcnamara KM, Vacanti JP, Langer R. Transplantation of hepatocytes using porous biodegradable sponges. *Transplant proc* 1994;26(6):3425–6.
- [5] Kaufmann PM, Heimarath S, Kim BS, Mooney DJ. Highly porous polymer matrices as a three-dimensional culture system for hepatocytes. *Cell transplant* 1997;6(5):463–8.
- [6] Qiang LV, Feng QL, Hu K, Cui FZ. Three-dimensional fibroin/collagen scaffolds derived from aqueous solution and the use for HepG2 culture. *Polymer* 2005;46(26):12662–9.
- [7] Madhally SV, Matthew HWT. Porous chitosan scaffold for tissue engineering. *Biomaterials* 2004;20(12):1133–42.
- [8] Khanna HJ, Klein MD, Matthew HWT. Novel design of a chitosan-collagen scaffold for hepatocyte implantation. Annual international conference of the IEEE engineering in medicine and biology-proceedings 2000; 2:1259–1298.
- [9] Kim UJ, Park J, Kim HJ, Wada M, Kalpan DL. Three-dimensional aqueous-derived biomaterial scaffolds from silk fibroin. *Biomaterials* 2005; 26(15):2775–85.
- [10] Hutmacher DW. Scaffold design and fabrication technologies for engineering tissues: state of the art and future perspectives. *J Biomater Sci Polym Ed* 2001;12:107–24.
- [11] Ishaug-Riley SL, Crane GM, Gurlek A, Miller MJ, Yasko AW, Yaszemski MJ, et al. Ectopic bone formation by marrow stromal osteoblasts transplantation using poly(DL-lactic-co-glycolic acid) foams implanted into the rat mesentery. *J Biomed Mater Res* 1997;36(1):1–8.
- [12] Freed LE, Vunjak-Novakovic G. Culture of organized cell communities. *Adv Drug Delivery Rev* 1998;33(1–2):15–30.
- [13] Holy CE, Shoichet MS, Davies JE. Bone marrow cell colonization of and extracellular matrix expression on biodegradable polymers. *Cell Mater* 1997;7:223–34.
- [14] Colton C. Implantable biohybrid artificial organs. *Cell Transplant* 1995; 4:415–36.
- [15] Folkman J, Hochberg M. Self-regulation of growth in three dimension. *J Exp Med* 1973;138:745–53.
- [16] Park A, Wu B, Griffith LG. Integration of surface modification and 3D fabrication techniques to prepare patterned poly(L-lactide) substrates allowing regionally selective cell adhesion. *J Biomater Sci Polym Ed* 1998;9:89–110.
- [17] Kim SS, utsunomiya H, Koski JA, WU BM, Cima MJ, Sohn J, et al. Survival and function of hepatocytes on a novel three-dimensional synthetic biodegradable polymer scaffold with an intrinsic network of channels. *Ann Surg* 1998;228(1):8–13.
- [18] Griffiths LG, Wu BM, Cima MJ, Powers MJ, Chaignaud B, Vacanti JP. *In vitro* organogenesis of liver tissue. *Ann NY Acad Sci* 1992;831:382–97.
- [19] Hutmacher DW, Schantz T, Zein I, Ng KW, Teoh SH, Tan KC. Mechanical properties and cell cultural response of polycaprolactone scaffolds designed and fabricated via fused deposition modeling. *J Biomed Mater Res* 2001;55:203–16.
- [20] Wang YD, Ammer GA, Sheppard BJ, Langer A. A tough biodegradable elastomer. *Nat Biotechnol* 2002;20(2):602–6.
- [21] Kaihara S, Borenstein JT, Koka R, Lalan S, Ochoa ER, Ravens M, et al. Silicon micromachining to tissue engineering branched vascular channels for liver fabrication. *Tissue Eng* 2000;6:105–17.
- [22] Shin M, Matsuda K, Ishii O, Terai H, Kaazempur-Mofrad M, Borenstein J, et al. Endothelialized networks with a vascular geometry in microfabricated poly (dimethyl siloxane). *Biomed Microdevices* 2004; 6(4):269–78.
- [23] Strain AJ, Neuberger JM. A bioartificial liver: state of the art. *Science* 2002;295:1005–9.

- [24] Griffith L, Naughton G. Tissue engineering—current challenges and expanding opportunities. *Science* 2002;295:1009–14.
- [25] Leclerc E, Furukawa KS, Miyata F, Sakai Y, Ushida T, Fujii T. Fabrication of microstructures in photosensitive biodegradable polymers for tissue engineering applications. *Biomaterials* 2004;25:4683–90.
- [26] Fidkowski C, Kaazempur-Mofrad MR, Borenstein J, Vacanti JP, Langer R, Wang YD. Endothelialized microvasculature based on a biodegradable elastomer. *Tissue Eng* 2005;11:302–8.
- [27] Shen F, Cui YL, Yang LF, Yao KD, Dong XH, Jia WY, et al. A study on the fabrication of porous chitosan/gelatin network scaffold for tissue engineering. *Polym Int* 2000;49:1596–9.
- [28] Yao KD, Xu MX, Yin YJ, Zhao JY, Chen XL. pH-sensitive chitosan/gelatin hybrid polymer network microspheres for delivery of cimetidine. *Polym Int* 1996;39:333–7.
- [29] Mao JS, Zhao LG, Yao KD, Shang QX, Yang GH, Cao YL. Study of novel chitosan-gelatin artificial skin *in vitro*. *J Biomed Mater Res* 2003;64A(2):301–8.
- [30] Mao JS, Zhao LG, Yin YJ, Yao KD. Structure and properties of bilayer chitosan-gelatin scaffolds. *Biomaterials* 2003;24:1067–74.
- [31] Li KG, Wang Y, Miao ZC, Xu DY, Tang YF, Feng MF. Chitosan/gelatin composite microcarrier for hepatocyte culture. *Biotechnol Lett* 2004;26:879–83.
- [32] Cheng MY, Deng JG, Yang F, Gong YD, Zhao NM, Zhang XF. Study on physical properties and nerve cell affinity of composite films from chitosan and gelatin. *Biomaterials* 2003;24:2871–80.
- [33] Elcin YM, Dixit V, Gitnick G. Hepatocyte attachment on biodegradable modified chitosan membranes: *in vitro* evaluation for the development of liver organoids. *Artif Organs* 1998;22(10):837–46.
- [34] Li JL, Pan JL, Zhang LG, Yu YT. Culture of hepatocytes on fructose-modified chitosan scaffolds. *Biomaterials* 2003;24:2317–22.
- [35] Lan S. Organ to order: researchers have high hopes of building an artificial liver. *New Sci* 2002;27:4–5.
- [36] Nazarov R, Jin HJ, Kaplan DL. Porous 3-D scaffolds from regenerated silk fibroin. *Biomacromolecules* 2004;5:718–26.
- [37] Zhang RY, Ma PX. Poly ( $\alpha$ -hydroxyl acids)/hydroxyapatite porous composites for bone-tissue engineering. I. Preparation and morphology. *J Biomed Mater Res* 1999;44:446–55.
- [38] Puviani AC, Ottolenghi C, Tassinari B, Pazzi P, Morsiani E. An update on high-yield hepatocyte isolation methods and on the potential clinical use of isolated liver cells. *Comp Biochem Phys A* 1998;120:99–109.
- [39] Rathke TD, Hudson SM. Review of chitin and chitosan as fiber and film formers. *Rev Macromol Chem Phys* 1994;C34:375–437.
- [40] Kojima K, Bonassar LJ, Roy AK, Mizuno H, Cortiella J, Vacanti CA. A composite tissue-engineered trachea using sheep nasal chondrocyte and epithelial cells. *FASEB J* 2003;17(8):823–8.
- [41] Metwalli AR, Colvert JR, Kropp BP. Tissue engineering in urology: where are we going? *Curr Urol Rep* 2003;4:156–63.
- [42] Oshima H, Inoue H, Matsuzaki K, Tanabe M, Kumagai N. Permanent restoration of human skin treated with cultured epithelium grafting-wound healing by stem cell based tissue engineering. *Hum Cell* 2002;15:118–28.
- [43] Yan YN, Wang XH, Pan YQ, Liu HX, Cheng J, Xiong Z, et al. Fabrication of viable tissue-engineered constructs with 3D cell-assembly technique. *Biomaterials* 2005;26:5864–71.
- [44] Moghe PV, Cogger RN, Toner M, Yarmuch ML. Cell-cell interactions are essential for maintenance of hepatocyte function in collagen gel but not on matrigel. *Biotechnol Bioeng* 1997;56(6):706–11.
- [45] Li JL, Pan JL, Zhang LG, Guo XJ, Yu YT. Culture of primary rat hepatocytes within porous chitosan scaffolds. *J Biomed Mater Res A* 2003;67:938–43.
- [46] Glicklis R, Shapiro L, Agbaria R, Merchuk JC, Cohen S. Hepatocyte behavior within three-dimensional porous alginate scaffolds. *Biotechnol Bioeng* 2000;67(3):344–53.
- [47] Yang J, Chung TW, Nagaoka M, Goto M, Cho CS, Akaike T. Hepatocyte-specific porous polymer-scaffolds of alginate/galactosylated chitosan sponge for liver-tissue engineering. *Biotechnol Lett* 2001;23:1385–9.
- [48] Chen JP, Lin TC. High-density culture of hepatocytes in a packed-bed bioreactor using a fibrous scaffold from plant. *Biochem Eng J* 2006;30:192–8.
- [49] Chung TW, Yang J, Akaike T, Chu KY, Nah JW, Kim SI, et al. Preparation of alginate/galactosylated chitosan scaffold for hepatocyte attachment. *Biomaterials* 2002;23:2827–34.
- [50] Eschbach E, Chatterjee SS, Noldner M, Gottwald E, Dertinger H, Weibezahn KF, et al. Microstructured scaffolds for liver tissue cultures of high cell density: morphological and biochemical characterization of tissue aggregates. *J Cell Biochem* 2005;95:243–55.
- [51] Powers MJ, Domansky K, Kaazempur-Mofrad MR, Kalezi A, Capitano A, Upadhyaya A, et al. A microfabricated array bioreactor for perfused 3D liver culture. *Biotechnol Bioeng* 2002;78:257–69.
- [52] Elcin YM, Dixit V, Lewin K, Gitnick G. Xenotransplantation of fetal porcine hepatocytes in rats using a tissue engineering approach. *Artif Organs* 1999;23(22):146–52.
- [53] Hunter SK, Kao JM, Wang Y, Benda JA, Rodgers VG. Promotion of neovascularization around hollow fiber bioartificial organs using biologically active substances. *ASAIO J* 1999;45(1):37–40.
- [54] Harada K, Mitaka T, Miyamoto S, Sugimoto S, Ikeda H, Mochizuki Y, et al. Rapid formation of hepatic organoid in collagen sponge by rat small hepatocytes and hepatic nonparenchymal cells. *J Hepatol* 2003;39:716–23.
- [55] Kidambi S, Sheng LF, Yarmush ML, Toner M, Lee I, Chan C. Patterned co-culture of primary hepatocytes and fibroblasts using polyelectrolyte multilayer templates. *Macromol Biosci* 2007;7:344–53.
- [56] Seo SJ, Kim IY, Choi YJ, Akaike T, Cho CS. Enhanced liver functions of hepatocytes cocultured with NIH 3T3 in the alginate/galactosylated chitosan scaffold. *Biomaterials* 2006;27:1487–95.
- [57] Bettinger CJ, Weinberg EJ, Kulig KM, Vacanti JP, Wang YD, Borenstein JT, et al. Three-dimensional microfluidic tissue-engineering scaffolds using a flexible biodegradable polymer. *Adv Mater* 2006;18:165–9.